

3D QSAR Study of 2-Methoxyphenylpiperazinylakanamides as 5-Hydroxytryptamine (Serotonin) Receptor 7 Antagonists

Santhosh Kumar Nagarajan and Thirumurthy Madhavan[†]

Abstract

5-hydroxytryptamine (serotonin) receptor (5-HT₇R) 7 is one of G-Protein coupled receptors, which is activated by the neurotransmitter Serotonin. After activation by serotonin, 5-HT₇ activates the production of the intracellular signaling molecule cyclic AMP. 5-HT₇ receptor has been found to be involved in the pathophysiology of various disorders. It is reported that 5-HT₇ receptor antagonists can be used as antidepressant agents. In this study, we report the important structural and chemical parameters for 2-methoxyphenylpiperazinylakanamides as 5-HT₇R inhibitors. A 3D QSAR study based on comparative molecular field analysis (CoMFA) was performed. The best predictions were obtained for the best CoMFA model with q^2 of 0.594 with 6 components, r^2 of 0.986, Fisher value as 60.607, and an estimated standard error of 0.043. The predictive ability of the test set was 0.602. Results obtained the CoMFA models suggest that the data are well fitted and have high predictive ability. The contour maps are generated and studied. The contour analyses may serve as tool in the future for designing of novel and more potent 5-HT₇R derivatives.

Keywords: 3D-QSAR, CoMFA, 5-HT₇R, Serotonin

1. Introduction

5-Hydroxytryptamine (serotonin) receptor (5-HT₇R) 7 belongs to the G-protein coupled receptor superfamily of cell surface receptors^[1]. It is activated by the Serotonin, a neurotransmitter. Serotonin receptors have been divided into seven families, 5-HT₁R to 5-HT₇R. 5-HT₇R is the recently cloned subtype of serotonin receptor family. After activated by serotonin, 5-HT₇ leads to a cascade of events starting with release of the stimulatory G protein G_s from the GPCR complex. This activates the production of cyclic AMP, an intracellular signaling molecule^[2]. It is expressed in a variety of human tissues, including brain, the gastrointestinal tract, and in various blood vessels^[3]. 5-HT₇ receptor plays important role in smooth muscle relaxation within the vasculature and in the gastrointestinal tract^[1]. It is involved in learning and memory, thermoregulation, circadian rhythm, and sleep. The 5-HT₇ receptor is

encoded by the HTR7 gene. The HTR7 gene is transcribed into 4 different splice variants, designated h5-HT_{7(a)}, h5-HT_{7(b)}, h5-HT_{7(c)} and h5-HT_{7(d)}^[4].

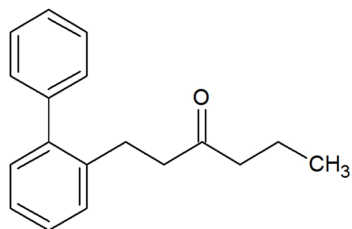
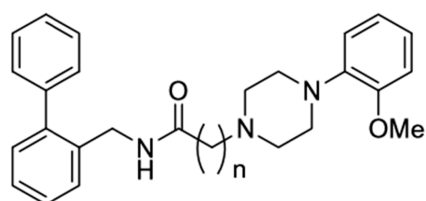
5-HT₇ receptor has been reported in the pathophysiology of various disorders. In recent times, 5-HT₇ receptor is in limelight because of its role in various neurological disorders including depression, sleep disorders, memory deficiency and neuropathic pain. They are also found to down regulate after antidepressant administration^[5]. These findings suggest that the 5-HT₇ receptor antagonists can be used as antidepressant agents^[6,7]. It is also reported that in animal models, 5-HT₇ receptor activation produced anti-hyperalgesic effects^[8]. It is also speculated that this receptor may be involved in mood regulation. This suggests that 5-HT₇ receptor can be a useful target in the treatment of depression^[9].

Various neutral antagonists and inverse agonists have been reported for 5-HT₇ receptor. Due to the differing levels of inverse agonist efficacy between receptor splice variants, differentiation between neutral antagonists and inverse agonists becomes complex. For example, mesulergine and metergoline, neutral antagonists of h5-HT_{7(a)} and h5-HT_{7(d)} receptor isoforms displays marked inverse agonist effects at h5-HT_{7(b)} splice variant^[10].

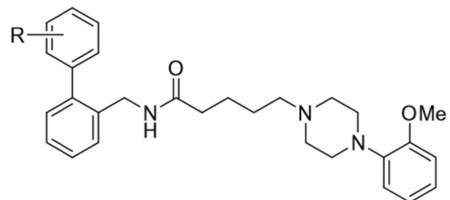
Department of Bioinformatics, School of Bioengineering, SRM University, SRM Nagar, Kattankulathur, Chennai 603203, India

[†]Corresponding author : thiru.murthyunom@gmail.com,
thirumurthy.m@ktr.srmuniv.ac.in

(Received: May 30, 2016, Revised: June 14, 2016,
Accepted: June 25, 2016)

Table 1. Structures and biological activities (pK_i) of 5-HT₇R inhibitors**The 2-methoxyphenylpiperazinyllakanamides inhibitor scaffold****a) Compound 1-4**

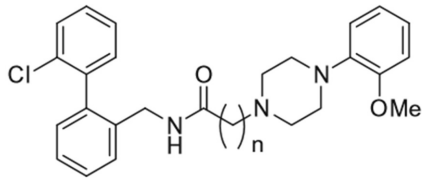
Compound	n	pK_i values
1*	2	6.729321
2	3	7.19044
3	4	7.421361
4	5	7.359519

b) Compound 5-17

Compound	R	pK_i values
5*	2'- F	7.437707
6*	3'- F	7.459671
7*	4'- F	7.459671
8	2'- Cl	8.06098
9	3'- Cl	6.392223
10	4'- Cl	7.5867
11	2'- OMe	7.50307
12	3'- OMe	7.657577
13*	4'- OMe	7.359519
14	2',6'- diOMe	7.489455
15	2'- Me	7.583359
16	3'- Me	7.322393
17	4'- Me	7.179799

Table 1. Continued

c) Compound 16-20



Compound	n	pK _i values
18*	3	7.331614
19	5	7.798603

*Test set compounds

It becomes apparent that there is a need for discovery of structurally diverse 5-HT₇ receptor antagonists for the treatment of various neurological disorders. Here, in this study, we report on the 3D-Quantitative structural activity relationship study on 2-methoxyphenylpiperazinylakanamides derivatives as 5-hydroxytryptamine (serotonin) receptor 7 antagonists.

2. Computational Methods

2.1. Data Set

The structures of the 2-methoxyphenylpiperazinylakanamides derivatives and the biological activities of 19 compounds were taken from the literature^[11]. K_i values of each inhibitor were converted into pK_i in order to use the data as dependent variable in CoMFA model. pK_i value is the negative logarithm of a K_i value. The test set molecules were selected which is the representative molecule for training set molecules. The test set molecules were selected manually so as to cover all the biological activity which is similar to the training set molecule. Compound 9 was omitted during the study as it was found to be an outlier. The total set of compounds was divided into a training set consist of 13 compounds and test set consist of 6 compounds. The structures and their activity values are displayed in Table 1.

2.2. Ligand-based Alignment Method

For each compound, the partial atomic charges were assigned by utilizing Gasteiger Hückel method available in SYBYLX 2.1 package (Tripos Inc., St. Louis, MO, USA). All rotatable bonds were searched with incremental dihedral angle from 120° by using system-

atic search conformation method. Conformational energies were computed with electrostatic term, and the lowest energy conformer was selected as template molecule. Then the template was modified for other ligands of the series. The common scaffold was constraint for each molecule and only the varying parts were energy minimized by Tripos force field with Gasteiger-Huckel charge by using conjugate gradient method, and convergence criterion was 0.05 kcal/mol at 10,000 iteration. Using the atom fit method; the minimized structures were aligned over the template (Fig. 1). Subsequently this alignment is used for 3D QSAR study based on Comparative molecular field analysis (CoMFA).

2.3. CoMFA Field Generation

SYBYLX 2.1 (Tripos Inc., St. Louis, MO, USA) package molecular modeling package was used for the 3D QSAR studies based on CoMFA. Generally used steric and electrostatic fields were used for this study. CoMFA studies helps in deriving a relation between the biological activities and three dimensional structures of the set of molecules of the dataset. The molecular alignment was placed in a 3D grid and the molecular field values of each conformation of a molecule are calculated. 2 Å lattice spacing was used. The CoMFA method was performed using steric and electrostatic fields with standard ±30 kcal/mol cutoffs. CoMFA calculated steric and electrostatic field values.

2.4. Partial Least Square (PLS) Analysis

PLS algorithm quantifies the relationship between the structural parameters and the biological activities^[12,13]. CoMFA descriptors used as independent variables and

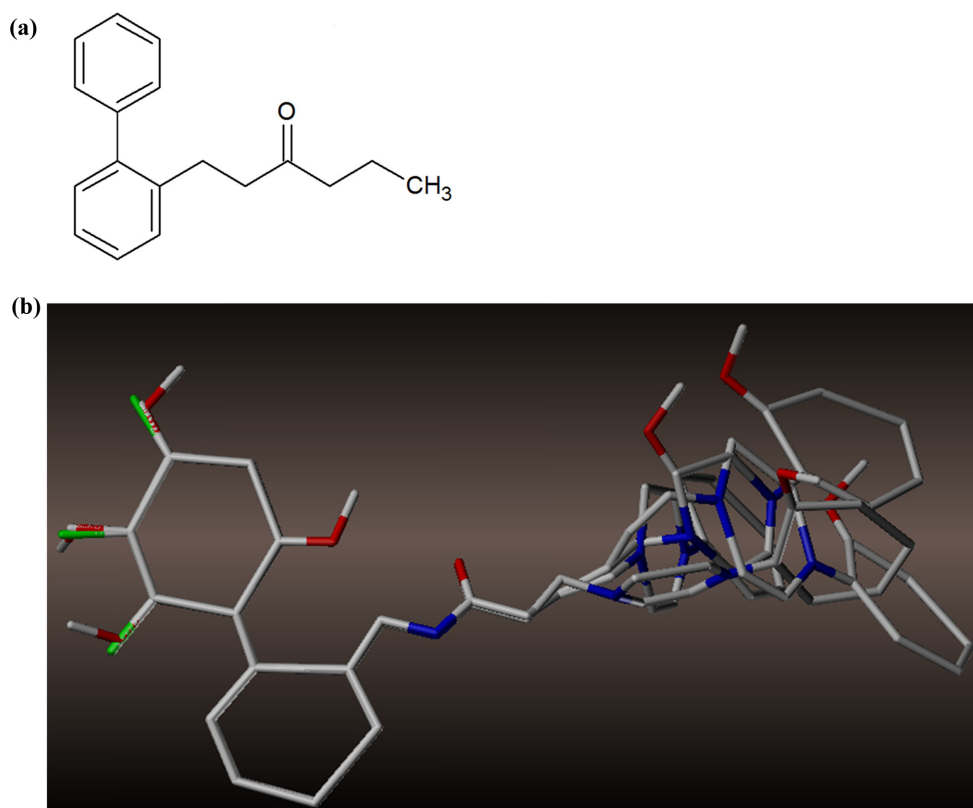


Fig. 1. (a) Maximum common substructure present in all molecules. (b) Alignment of molecules based on systematic search conformation of highly active compound 8.

pK_i values used as dependent variables in PLS analysis for the generation of 3D-QSAR models. Leave-one-out (LOO) cross-validation procedures were used to obtain the cross-validated correlation coefficient (q^2), non-cross-validated correlation coefficient (r^2), standard error estimate (SEE) and Fisher's values (F)^[14,15]. A non-cross-validated analysis was carried out without column filtering was then followed. The cross-validated correlation coefficient (q^2) was calculated using the following equation:

$$q^2 = 1 - \frac{\sum_{\gamma} (\gamma_{pred} - \gamma_{actual})^2}{\sum_{\gamma} (\gamma_{actual} - \gamma_{mean})^2}$$

where γ_{pred} , γ_{actual} , and γ_{mean} are the predicted, actual, and mean values of the target property (pK_i), respectively.

The predictive power of CoMFA models were deter-

mined from the set of seven test molecules which was excluded during model development. The predictive correlation coefficient (r_{pred}^2) based on the test set molecules, is defined as:

$$r_{pred}^2 = \frac{(SD - PRESS)}{SD}$$

where PRESS is the sum of the squared deviation between the predicted and actual activity of the test set molecules, and SD is defined as the sum of the square deviation between the biological activity of the test set compounds and the mean activity of the training set molecules.

3. Results and Discussion

3.1. CoMFA Analysis

CoMFA models were derived with the combination of steric and electrostatic field contributions and

Table 2. Statistical results of CoMFA models obtained from systematic search conformation based alignment

PLS statistics	Ligand-based CoMFA model (Systematic search conformation based alignment)				
	Model 1	Model 2	Model 3	Model 4	Model 5
q ²	0.568	0.564	0.594	0.492	0.528
N	6	6	6	6	6
r ²	0.985	0.984	0.986	0.968	0.986
SEE	0.046	0.0047	0.043	0.067	0.044
F-value	55.085	50.348	60.607	25.353	59.326
r ² _{pred}	0.512	0.507	0.602	0.452	0.484
Field contribution					
Steric	0.486	0.459	0.469	0.451	0.476
Electro static	0.514	0.541	0.531	0.549	0.524

q²= cross-validated correlation coefficient; N= number of statistical components; r²= non-cross validated correlation coefficient; SEE=standard estimated error; F=Fisher value; r²_{predictive}= predictive correlation coefficient for test set.

The model chosen for analysis is highlighted in bold fonts.

Test set compounds

Model 1- compound no 1, 5, 6, 7, 15, 18

Model 2- compound no 1, 5, 6, 7, 12, 18

Model 3- compound no 1, 5, 6, 7, 13, 18

Model 4- compound no 1, 5, 6, 7, 10, 18

Model 5- compound no 1, 5, 6, 10, 15, 18

Table 3. Predicted activities and experimental pK_i values obtained from CoMFA models

Compound	Actual pK _i	Predicted	Residual
1*	6.729321	7.345	-0.6157
2	7.19044	7.188	0.0024
3	7.421361	7.505	-0.0836
4	7.359519	7.332	0.0275
5*	7.437707	8.211	-0.7733
6*	7.459671	8.048	-0.5883
7*	7.459671	7.747	-0.2873
8	8.06098	8.025	0.0360
10	7.5867	7.598	-0.0113
11	7.50307	7.502	0.0011
12	7.657577	7.649	0.0086
13*	7.359519	7.351	0.0085
14	7.489455	7.468	0.0215
15	7.583359	7.401	0.1824
16	7.322393	7.31	0.0124
17	7.179799	7.177	0.0028
18*	7.331614	7.68	-0.3484
19	7.798603	7.824	-0.0254

*Test set compounds

Gasteiger-Hückel charge method with 2.0 Å grid space. Different combinations of training and test compounds were used for model generation. Based on the reliable q² and r²_{pred} values, 5 best models were selected out of the number of models created. The statistical values of the 5 models are tabulated in Table 2. Leave one out (LOO) analysis gave a cross-validated q² of 0.594 with 6 components and non cross-validated PLS analysis resulted in a correlation coefficient r² of 0.986, Fisher value as 60.607, and an estimated standard error of 0.043. The predictive ability of the developed CoMFA model was assessed by the test set predictions, which were excluded during model generation. The predictive ability of the test set was 0.602. Predicted and experimental activities and their residual values of all inhibitors are shown in Table 3, and the corresponding scatter plot is depicted in Fig. 2.

3.2. CoMFA Contour Map

Contour maps were generated based on the CoMFA analyses. The maps are represented as regions in 3D space. In these maps, the changes in the steric and electrostatic fields of a compound correlate strongly with changes in its biological activity. A scalar product of

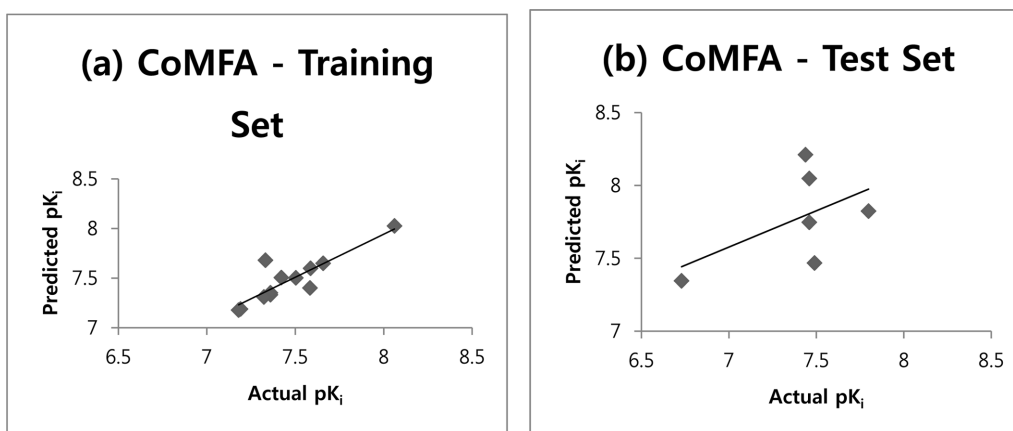


Fig. 2. (a and b) Plot of actual versus predicted pK_i values for the training set and test set for the CoMFA values performed after atom-by atom matching alignment by systematic search.

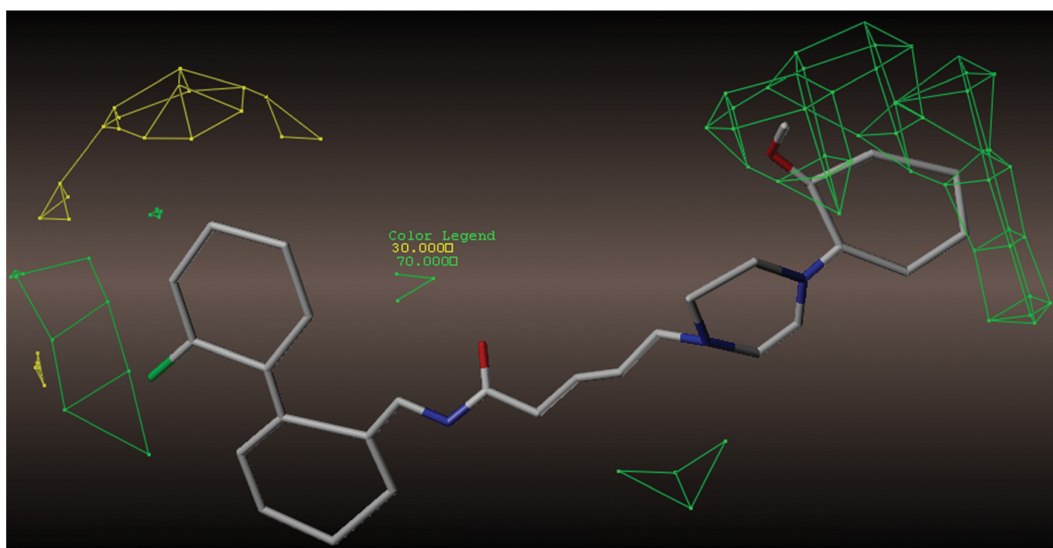


Fig. 3. CoMFA steric contour map with highly active compound 8 for systematic search based alignment. Green contour indicates region where bulky group increases activity and yellow contours indicates bulky group decreases activity.

coefficients and standard deviation ($SD \cdot Coeff$) associated with each column were generated as contour maps. Favored levels were fixed at 70% and disfavored levels were fixed at 30%.

Based on the ligand-based (atom-by atom matching) alignment method, CoMFA contour maps were generated. The result is represented as a 3D 'coefficient contour' map. The steric contour map is represented in Fig. 3. Here, green color in the steric contour maps depicts the more bulk molecules favored region whether yellow

color region represent the less bulk molecules favored in the region. The green steric contour near the R position of the phenyl ring indicates that substitution of bulky group is preferred at this position. Compounds 8, 15, 18 and 19 have bulkier substituents at this position, hence they are more active. There was a yellow contour region near to the green contour map; which indicates that substitution of bulkier groups would decrease the activity. This may be the reason why the compounds 13 and 17 having bulkier substitution shows less activity.

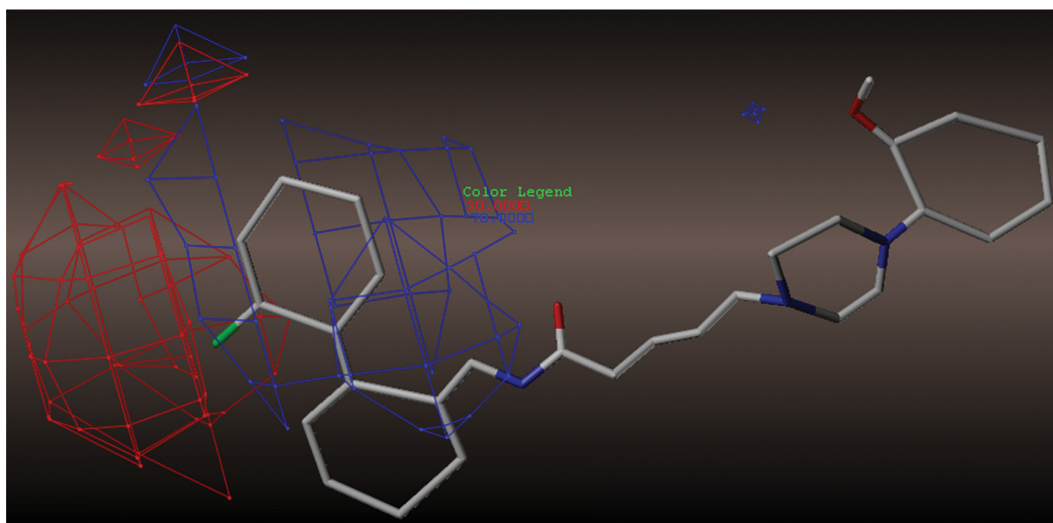


Fig. 4. CoMFA electrostatic contour map with highly active compound 8 for systematic search based alignment. Blue contour indicates regions where electropositive groups increases activity and red contours indicates regions where electronegative groups increases activity.

Fig. 4 represents the electrostatic contour map. In electrostatic field contours, red regions represent electronegative substituents favored regions and blue regions represent electropositive substituents favored regions. The plot shows a blue colored region situated surrounding the R positions of 7, 10, 13 and 17. Here the electropositive charges in these regions are very important for ligand binding, and electropositive group linked to this position will enhance the biological activity. A red contour region is present at the R position of 5, 8, 11, 14 and 15. In these positions the electronegative groups increases activity.

4. Conclusion

A reliable 3D-QSAR model from 2-methoxyphenylpiperazinylakanamides derivatives as 5-hydroxytryptamine (serotonin) receptor 7 antagonists was developed using CoMFA method based on atom-by-atom matching alignment. Important steric and electrostatic sites that can influence the bioactivities of the compounds were represented using the CoMFA contour maps. From steric contour maps, it is found that the substitution of bulkier groups in the R position enhances the biological activity. Yellow contour region indicated that the substitution of bulkier groups in the R position would decrease the activity. The electrostatic contour

map showed that the substitution of electron donating group in R position improves the biological activity. These results can enlighten the important structural and chemical features in developing new potent and novel inhibitors for 5-hydroxytryptamine (serotonin) receptor 7.

References

- [1] P. Vanhoenacker, G. Haegeman, and J. E. Leysen, "5-HT7 receptors: current knowledge and future prospects", *Trends Pharmacol. Sci.*, Vol. 21, pp. 70-77, 2000.
- [2] M. Ruat, E. Traiffort, R. Leurs, J. Tardivel-Lacombe, J. Diaz, J. M. Arrang, and J. C. Schwartz, "Molecular cloning, characterization, and localization of a high-affinity serotonin receptor (5-HT7) activating cAMP formation", *P. Natl. Acad. Sci. U.S.A.*, Vol. 90, pp. 8547-8551, 1993.
- [3] J. A. Bard, J. Zgombick, N. Adham, P. Vaysse, T. A. Branchek, and R. L. Weinshank, "Cloning of a novel human serotonin receptor (5-HT7) positively linked to adenylate cyclase", *J. Biol. Chem.*, Vol. 268, pp. 23422-23426, 1993.
- [4] D. Hoyer, D. E. Clarke, J. R. Fozard, P. R. Hartig, G. R. Martin, E. J. Mylecharane, P. R. Saxena, and P. P. Humphrey, "International Union of Pharmacology classification of receptors for 5-hydroxytrypt-

- amine (Serotonin)", *Pharmacol Rev.*, Vol. 46, pp. 157-203, 1994.
- [5] J. P. P. Foong and J. C. Bornstein, "5-HT antagonists NAN-190 and SB 269970 block alpha2-adrenoceptors in the guinea pig", *Neuroreport*, Vol. 20, pp. 325-330, 2009.
- [6] G. Sarkisyan, A. J. Roberts, and P. B. Hedlund, "The 5-HT(7) receptor as a mediator and modulator of antidepressant-like behavior", *Behav. Brain Res.*, Vol. 209, pp. 99-108, 2010.
- [7] O. Mnie-Filali, C. Faure, L. Lambás-Señas, E. M. Mansari, H. Belblidia, E. Gondard, A. Etiévant, H. Scarna, A. Didier, A. Berod, P. Blier, and N. Hadjjeri, "Pharmacological blockade of 5-HT7 receptors as a putative fast acting antidepressant strategy", *Neuropsychopharmacol.*, Vol. 36, pp. 1275-1288, 2011.
- [8] G. S. Perez-García and A. Meneses, "Effects of the potential 5-HT7 receptor agonist AS 19 in an autoshaping learning task", *Behav. Brain Res.*, Vol. 163, pp. 136-140, 2005.
- [9] V. S. Naumenko, N. K. Popova, E. Lacivita, M. Leopoldo, and E. G. Ponimaskin, "Interplay between serotonin 5-HT1A and 5-HT7 receptors in depressive disorders". *CNS Neurosci. Ther.*, Vol 20 pp. 582-590, 2014.
- [10] K. A. Krobert and F. O. Levy, "The human 5-HT7 serotonin receptor splice variants: constitutive activity and inverse agonist effects", *Brit. J. Pharmacol.*, Vol 135, pp. 1563-1571, 2002.
- [11] Y. Kim, J. Tae, K. Lee, H. Rhim, I. H. Choo, H. Cho, W.-K. Park, G. Keum, and H. Choo, "Novel N-biphenyl-2-ylmethyl 2-methoxyphenylpiperazinyllakanamides as 5-HT7R antagonists for the treatment of depression", *Bioorgan. Med. Chem.*, Vol. 22, pp. 4587-4596, 2014.
- [12] S. J. Cho and A. Tropsha, "Cross-validated R2-guided region selection for comparative molecular field analysis: A simple method to achieve consistent results", *J. Med. Chem.*, Vol. 38, pp. 1060-1066, 1995.
- [13] S. Wold, M. Sjostrom, and L. Eriksson, "PLS-regression: a basic tool of chemometrics", *Chemometr. intell. lab.*, Vol. 58, pp. 109-130, 2001.
- [14] U. Debnath, S. Verma, S. Jain, S. B. Katti, and Y. S. Prabhakar, "Pyridones as NNRTIs against HIV-1 mutants: 3D-QSAR and protein informatics" *J. Comput. Aid. Mol. Des.*, Vol. 27, pp. 637-654, 2013.
- [15] D. Fernández, J. Ortega-Castro, and J. Frau, "Human farnesyl pyrophosphate synthase inhibition by nitrogen bisphosphonates: A 3D-QSAR study" *J. Comput. Aid. Mol. Des.*, Vol. 27, pp. 739-754, 2013.